ISSN 1454 - 8003
Proceedings of 2023 International Conference on Hydraulics and Pneumatics - HERVEX
November 8-10, Băile Govora, Romania

COLD SPRAYED Ti-6Al-4V COATINGS ON HYDRAULIC COMPONENTS

Wojciech ŻÓRAWSKI[1], Rafał CHATYS[1], Medart MAKRENEK[2], Dominika SOBOŃ[1]

[1] Kielce University of Technology, Faculty of Mechatronics and Mechanical Engineering, e-mail: ktrwz@tu.kielce.pl; chatys@tu.kielce.pl; dsobon@tu.kielce.pl

[2] Kielce University of Technology, Faculty of Management and Computer Modeling, e-mail: fizmm@tu.kielce.pl

Abstract: *Cold Spraying (CS) is a thermal spray process investigated and presented by many authors as an alternative to producing AM freeform parts. It has severe differences from the laser, welding, and other thermal spray processes since CS does not change the properties of the feedstock powder by heating or melting during the AM part fabrication because the powder is kept below its recrystallization temperature during the spraying time. However, CSAM produces parts with a very high density, >99%, due to the very high velocity imposed on the particles, reaching supersonic velocity values. Therefore, the correct selection of feedstock powder, deposition parameters, and strategy are fundamental for achieving high Deposition Efficiency (DE) and good CSAM performance. CS also prevents materials oxidizing during the deposition due to the relatively low temperature that the material absorbs at the spraying time. In addition, CS avoids other harmful effects seen in other AM or thermal spray processes, such as evaporation, melting, recrystallization, tensile residual stresses, debonding, and gas releasing, besides the ability to deposit high-reflective metals such as Cu and Al. A great CSAM advantage is the possibility of the deposition of dissimilar materials, e.g., a sandwich-like structure of Cu and Al or composite components, which is not feasible by welding. The performed statistical analysis of the components determined the complexity of the layered composite structure. And the developed model of the weakest micro-volume presented in this work was the basis for describing not only the predictable strength of the laminate, but also the character of failure, taking into account the stresses in the reinforcement and the distribution of final deformations in the structure of the composite under consideration.*

Keywords**:** *Cold sprayed, the cross-linking process, component of composite, strength*

1. Introduction

The process of depositing metal coatings on polymers or more complex engineering materials such as plastics to obtain good strength properties at the expense of less weight (in many industries) is a topical subject. The process is valuable for depositing materials that are extremely sensitive to the presence of oxygen and readily oxidize at moderately elevated temperatures. Examples of oxygen-sensitive coatings that are typically produced by cold spraying: composites of aluminum, copper, titanium and carbides (e.g., tungsten carbide), as well as coatings made from amorphous alloys.
The wide assortment of composite components (especially those with a polymer matrix) appearing on the market, forces us to develop new models and procedures for molding the strength properties and resin systems, respectively, in the manufacture of laminate.
During the crosslinking of chemically curable compounds such as epoxy resins (with the structure of polar epoxy rings) having the nature of polyaddition (or ionic polymerization), the curing process proceeds without volatile by-products (low-molecular-weight precipitates), based on bisphenol A glycidyl ether (DGBEA - diglycidyl ether of bisphenol A [1-3]. That's why the curing process is so important, determining the quality of the laminate and its adhesion with other materials. And non-uniform curing as a result of failure to meet the reaction parameters (non-linear increase in internal temperature due to exothermic chemical reaction of epoxy), leads to exceeding the so-called "life of the resin system" and may cause incomplete curing or entrapment of volatiles or voids, respectively, and thus degradation of the matrix.
Among other things, cold spraying can be used to repair machine parts to (metal particles, nickel alloys or titanium alloys move in a mixture of nitrogen and helium and are gradually applied to the damaged part) restore the desired surface. That is, in this process, metal powder with relatively small particles (1÷50 μm in diameter) is applied to the coating. Additional heating of the batch powder does

not occur, unlike other thermal spraying processes. Particles of powder carried from powder feeder by separate gas stream are injected into a high velocity stream of the gas (300÷1200 m/s) and accelerated towards substrate. The stream of the pressurised and preheated gas achieves high velocity by flowing through a converging-diverging nozzle. In the diverging part of the nozzle gas is expanded to supersonic velocity with simultaneous fall of pressure and temperature. The particles are first injected in front of the nozzle throat or downstream and after exiting the nozzle impact onto substrate at a very high speed (Fig. 1). Upon impact, the particles in the solid state (opposite to the others thermal spray processes where particles after heating are plastic or molten) deform to the form of the splat and create a bond with the substrate. Subsequent new particles impact onto the substrate and form bonds with previously sprayed and deformed particles. Because of very high speed of powder particles, despite the lack of heating, the degree of particles deformation is very high. As a result, a uniform coating with small number of pores and a very high adhesion and cohesion are formed. The definition “cold spray” has come into being to describe this process due to low temperatures (-100 ÷ 100 ^{o}C) of the gas stream at the exit of the nozzle.

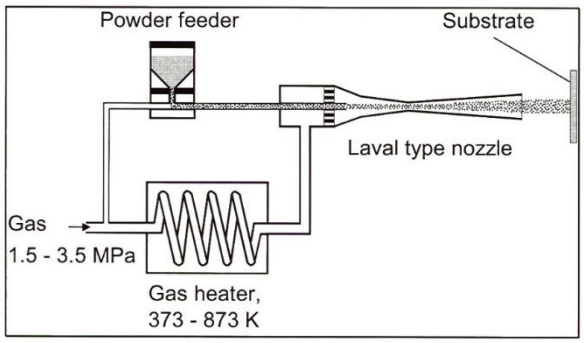

Fig. 1. Schematic of cold spray [4]

The basic characteristic feature of cold spray process is the temperature of the gas stream which is always below the melting point of the sprayed material. As a result, the coating is formed in a solid state. All phenomena accompanying creating of the coating as adhesion to the substrate or cohesion are accomplished in a solid state too, so cold sprayed coatings present unique properties. Firstly, low temperature of the process lets to avoid any phase changes in the feedstock powder, so the sprayed coating presents the same phase composition. Next, as other deleterious phenomena as particle oxidation, evaporation, melting, recrystallisation or gas release are avoided, the obtained coatings are more durable with a better bond strength. Additionally, a very strong adhesion of the coatings to the substrate occurs as result of low temperature of coating deposition.
The objective of the presented studies was to analyze the microstructure and mechanical properties of a cold sprayed Ti-6Al-4V structure for the structure of a composite (laminate) for application in additive manufacturing on hydraulic components.

2. Experimental Data Processing

2.1 Component selection and composite manufacturing technology

In order to carry out the task at hand, that is, spraying a layer of Ti-6Al-4V onto a 4-layer composite molded by the Vacuum Bagging Method at the laboratory of Kielce University of Technology. The flexible vacuum bagging method [5, 6] involves extracting excess resin system and air from a package of percolated composite reinforcement between the mold and the vacuum bag.
In the composite molded by vacuum methods, a 200g/m^3 carbon fabric reinforcement [7] and LH 288 epoxy resin (with H 505 hardener) were selected. The bisphenol A-based epoxy matrix is characterized by very low viscosity, excellent mechanical and chemical properties and thermal strength.

2.2 Vacuum forming process of layered composite

It should be mentioned that at the initial stage of layered composite manufacturing, the mold was degreased by applying a thin layer of a separator (such as Spacewax 300). After the acetone evaporated from the separator (after about 15 - 20min), the surface of the mold was polished (in order to achieve a better quality of the mold surface). After which, double-sided adhesive tape was applied to the edges of the mold, thus defining the field of the prepared mold.
Then, after the appropriate number of layers of carbon cloth were applied and seeped, auxiliary materials were applied (Table 1) and the flexible bag was fixed with clamps on the edges of the mold. An attached spigot (with a vent and optional vacuum reading connector installed), extracted air and possibly excess resin system from the laminate using a vacuum pump.

Table 1: Results of tests of static strength component composites [8]

No	Supporting material	Functions
1	Delamination (peel ply)	acting as a separator of the final product, after tearing off provides a matt laminate surface 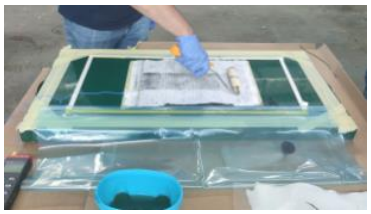
2	suction mat (breathable)	which extracts excess resin system 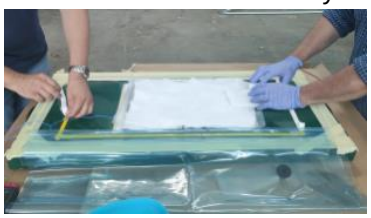
3	perforated foil	which is stuck to the edge of the mould with double-sided tape (Fig. 4), thus creating a vacuum (closed system) 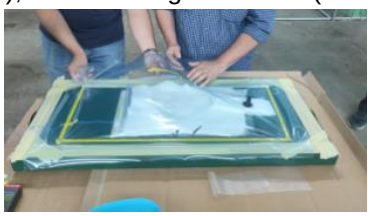

The process of introducing the resin system (injection molding) in a liquid state is carried out through the feed channels into the mold, which were closed after 13 minutes. The technological parameters of the molded laminate with a percentage of 50/50 components are shown in Table 2.

Table 2: Technological parameters of layered composite obtained using vacuum bagging method

Pressure, bar	**Hardener**	**Molding time,h**	**Gelation time, h**	**Additional heating, °C(h)**
- 0.6 overpressure	27% H 505	ca. 24	1.5 (*T*=21-23°C)	50 (10

Then, samples according to PN-EN 10002-1+ACI were cut out of the carbon-epoxy laminate with an average thickness of 1.8 2.0 mm, with dimensions (250 x 25mm) and a 200mm measuring base. The cut specimens were then subjected to a static tensile test on a SHIMADZU AGX-V 20kN machine at a speed of 2 mm/min.

To determine the effect of post-curing, the rest of the specimens were then exposed to UV lamps at 60°C (with 0.76W-m-2 ×nm^{-1} light at 340nm wavelength) and an additional annealing at 50°C for 4h in accordance with ISO 4892-3 and the manufacturer's recommendations.

2.3 Methodology

The coatings were sprayed using the Impact Innovations 5/8 system with the robot Fanuc M-20iA at Kielce University of Technology [9]. The feedstock used for this study was commercial Ti-6Al-4V powder with a "coral-like" morphology (Fig. 2). The working gases used in this process were nitrogen and helium in equal proportions. The coatings sprayed onto the titanium mandrel had a thickness of 15 mm. The microstructure and chemical composition of the powder and the coating were analyzed by means of SEM Jeol JSM-7100. The micromechanical testing of coatings was carried out with the use of the nanoindentation technique (Nanovea) with a Berkovitz indenter (the Olivier and Pharr methodology).

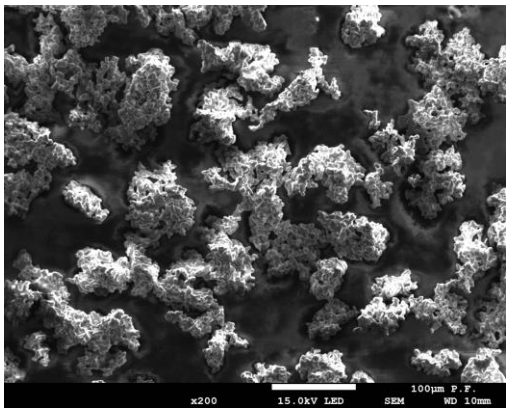

Fig. 2. Morphology of Ti-6Al-4V powder

The high kinetic energy of feedstock particles and their morphology caused significant deformation, and particular splats strongly adhered to the substrate and to each other. Throughout the cross-section, the coating was homogenous and exhibited negligible porosity (Fig. 3).

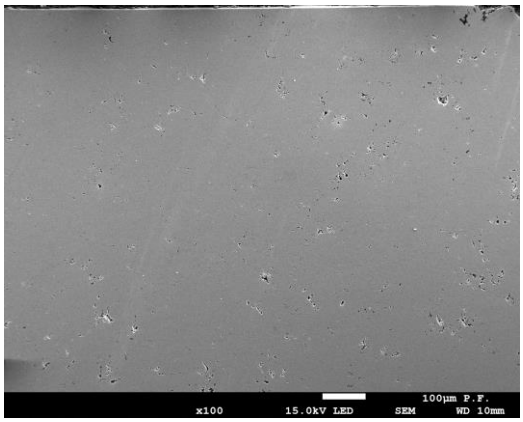

Fig. 3. Microstructure of cold sprayed Ti-6Al-4V coating

On the other hand, histograms and probability distributions of the hardness and Young's modulus of cold sprayed coating showed significant differences (Fig. 4).

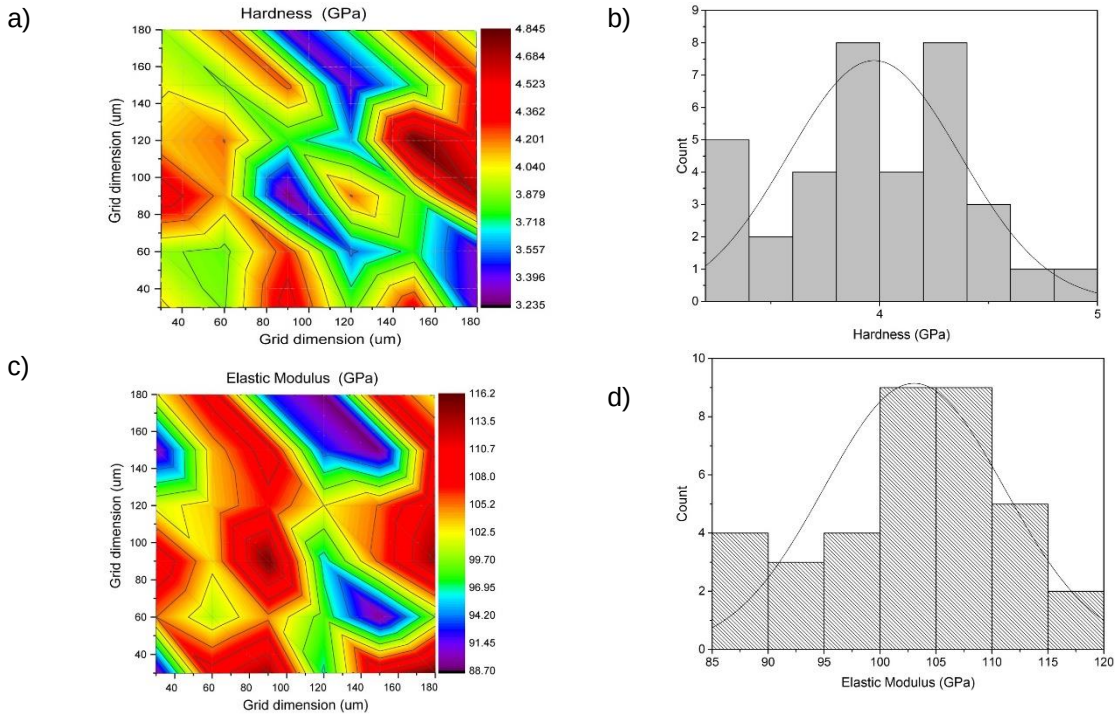

Fig. 4. Distribution of the mechanical properties for a Ti-6Al-4V cold spray coating: (a) hardness map, (b) hardness histogram, (c) elastic modulus map, (d) elastic modulus histogram

2.3.1 Statistical analysis of laminate (sandwich composite) components

The processing of experimental data was based on the assumption that the strength of samples of fibers, bundles of fibers, respectively, decreases as the complexity of the structure increases (which takes into account the strength properties of the components).

$$\sigma_{\text{fibres}} > \sigma_{\text{bundels of fibres}} > \sigma_{\text{sandwich composite (laminate)}} \quad (1)$$

To this end, the distribution function of the glass composite components [10] was investigated as a result of static tensile testing for 12 and 64 samples (Fig. 5) of fibres and an elementary fibre bundle (so-called strands consisting of 10 fibres), respectively. When analysing the experimental data, it is quite important to determine the magnitude of the scatter and to adopt a hypothesis regarding the statistical distributions of the static strength (S_{static}) of the components of the analysed composite structure. Then, the hypothesis of log.-normal strength distribution [19] was adopted for the tested samples through the function:

$$y(x) = x(1 - \Phi_0((\log(x) - \theta_0)/\theta_1)) \quad (2)$$

where $\Phi_0(\cdot)$ - is the standard normal distribution function.

The complexity of the structure of the composite material (from the fibre to the fibre-strand bundle, and then to the laminate itself) causes a deterioration of the average strength and a change in the parameters of the strength probability distribution function (showing a reduction in the value of the statistical parameter which is the standard deviation). Fig. 5 shows classical probability plots of the static strength of the composite components as well as of the composite itself. It can also be seen that the strength range of the fibre bundle specimens is much larger than the strength range for the epoxy composite. This is because no two identical active fibres can ever be obtained, as each bundle has a different number of broken fibres that do not carry the load. Assuming in the model (the main idea of the Daniels model) that the distribution of tensile loads S between n parallel, uninterrupted composite components (strands or fibres) is uniform with the expected fraction of failed strands S_b (the average nominal breaking strength) will be equal to F(s), where F(.) is a function of the cumulative strength distribution of the n strand bundle.

$$s_b = \max_s n \cdot s(1 - F(s)) \tag{3}$$

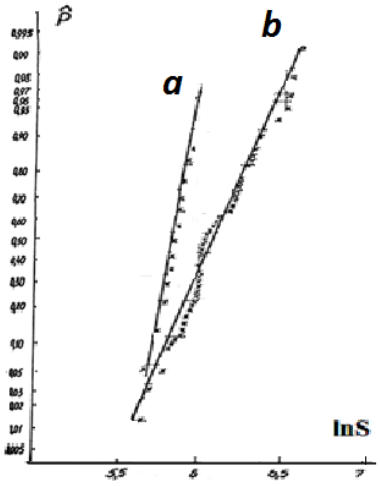

Fig. 5. The normal plot for static strength of a – specimens, b – 10 strands [11]

Making the above assumptions in accordance with the idea of the Daniels model, it can be formulated that: "all fibres have the same load-stress curve and b(S) is the probability of failure of one fibre under load S and (1-b(S)) converges to 0 faster than 1/S, then the strength of a strand S with a sufficiently large number of fibres has a normal distribution with an expectation value, whose parameters are shown in Table 3.

Table 3: Parameters of the probability distribution function of the composite strength

No.	Parameters	Correlations
1	Normal distribution with expected value	$S_r = n \cdot s_r \cdot [1 - b(s_r)]$ (4)
2	Standard deviation (OS)	$\sigma = s_r \cdot \sqrt{n \cdot b(s_r) \cdot [1 - b(s_r)]}$ (5) where: s_r corresponds to the maximum $s \cdot [1 - b(s)]$, which is the average force $\bar{S}_r = s_r \cdot [1 - b(s_r)]$ then OS has the form: $\bar{\sigma} = s_r \cdot \sqrt{b(s_r) \cdot [1 - b(s_r)]} / \sqrt{n}$ (6)

3. A strength model of a fibrous composite with statistical analysis of the properties of polymer matrix components sprayed with Ti-6Al-4V

Assuming a composite consisting of n-fibres embedded in a matrix and the assumptions in Table 4, we observe damage to components within elementary micro-volumes as a result of the development of micro-destruction (elementary volume through the destruction of individual fibres, fibre bundles, matrix cracks up to the avalanche development of macro-cracking).

Table 4: Results of tests of static strength component composites [8]

No	Model objectives
1	The composite consists of fibres (processed into fibre bundles) and matrix, as monolithic joints (Fig. 6).

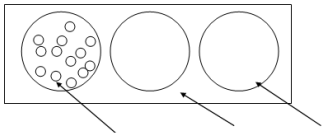

Fig. 6. Fiber bundles immersed in a matrix: 1 - fibers, 2 - matrix, 3 - bundles of fibers

2 The fibres (fibre bundles) have random physical-mechanical properties with randomly distributed defects.

3 The deformation in the cross-section is the same in all elements (i.e. the stress in the matrix is less than that in the fibre bundles and the shear deformation in the bundles is negligible compared with the shear deformation in the matrix).

4 When a fibre or a bundle of fibres in a layer (or sandwich composite) breaks, it is transferred to the adjacent fibres (bundles) as a result of shear forces in the matrix (Fig. 7).

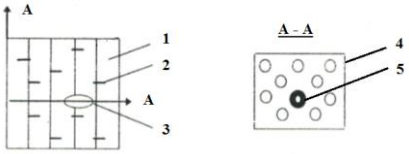

Fig. 7. Composite: 1 - bundles, 2 - matrix, 3 - crack bundles, 4 - elementary destruction volume, 5 – destroyed

5 The accumulation of damage cracks in the material structure leads to the appearance of a sufficient number of non-functioning fibre segments (bundles) in the whole volume and the formation of weak segments, which leads to the destruction of the layer (and the laminate) through a critical elementary volume L_{kr} (Fig. 8).

$$L_{kp} = d_f \left[\left(\frac{1-V_f^{0.5}}{V_f^{0.5}}\right)\frac{E_f}{G_m}\right]^{0.5} arch\left[\frac{1-(1-\varphi)^2}{2(1-\varphi)}\right], \quad (7)$$

where: L_{kp} - critical ineffective length; j φ - is the relative loading level at which the fiber is considered included in the work (0.97); d_f - is the fiber diameter; E_f - is the elastic modulus of the fiber; G_m - matrix shift modulus; V_f - is the filling factor.

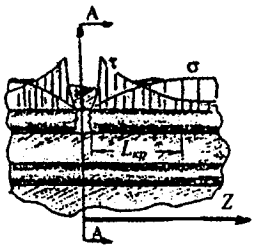

Fig. 8. Elementary volume with broken fibre at ineffective length (lkr) at tension (τ, σ)

6 The destruction process takes place in the same way in both the resin bond and the sandwich composite (laminate).

4. Analysis of the results

The obtained values of strength (σ) of the 4-layer composite (from static tensile testing), highlight a slight deviation from the average σ = 126.20MPa (Table 5), related to the plasticization of the matrix. The source of this behavior is their complex microstructure, which makes polymers at the molecular level (i.e. chains, network rings and their crystalline, amorphous and mixed combinations) sensitive to the effects of temperature, visible and ultraviolet light, as well as water (moisture), atmospheric and chemical pollutants.

Table 5: Mechanical properties of the layered composite obtained by the vacuum bagging after accelerated postconditioning of the laminate with fluorescent light in parts of the UVA, UVB and UVC spectrum

Sample No.	ε, mm	σ_{max}, MPa	E, GPa
A–1	1.60	110.47	6.56
A–2	1.84	121.96	6.65
A–3	2.14	146.17	6.76
average	1.85	126.20	6.65

Assuming that the given arrangement of reinforcements works to a greater extent in shear, the glass reinforcement will be destroyed earlier as a result of shearing of the interfacial boundary and the resin layer between the layers, causing significant changes in material constants depending not only on the strength of components (fibres and matrix), but also on the course of the technological process (uneven fibre arrangement in the whole volume, local discontinuities of fibres, lack of adhesion at the fibre - matrix boundary, as well as voids, micro-cracks or gaps) and additional matrix plasticisation. With a view to a uniform stress distribution in the volume.

$$\sigma = \frac{P}{\phi \cdot F_i \cdot n_i} \tag{8}$$

where: n_i - number of fibers, (i = 1, 2, 3,..., n); F_i - cross-sectional surface area pole of the fibre;
P - force (load); Φ - the load level at which the fibre effectively works with the matrix.
The destruction of components (fibres and fibre bundles with individual physical-mechanical properties [12, 13] was based on the critical micro volume.
The location of torn components as fibres, (or bundles of fibres) is random causing an increase of loads between them. At the destruction of the reinforcement in the composite structure the mechanism of stress distribution between the adjacent components (fibers, or fiber bundles) on L_{kr} is activated (under the influence of tangential stresses τ, regroups the stresses on the adjacent fibers - Fig. 3).

$$\tau_{lok} = \frac{\beta\, r}{2} \cdot \varepsilon\ E_i \tanh\left(\frac{\beta\, l}{2}\right) \tag{9}$$

where β – const. ($\beta = \frac{1}{B}$); ε – fibre elongation of the i-th component of the composite;
r – fibre radius, l – fibre length (critical length).
Where:

$$\tanh(x) = \frac{e^x - e^{-x}}{e^x + e^{-x}} \tag{10}$$

The failure process continues, as the load on the fibre is increased by the amount of the redistributed portion of the stress from the broken fibre (or fibre bundle). If the ultimate strength of the laminate (fibre bundle) is exceeded, the redistribution of local stresses (between adjacent components) is not possible.
In such a case the failure of the n^{-th} volume (V_n) with already significant de-lamination takes place in the weakest micro-volume, which is the strength criterion of the whole laminate (Table 6).

$$\sigma = 2\tau/\beta r \tag{11}$$

Table 6: Parameters of the model taking into account the crosslinking process (post-curing) of the laminate

Cross-referencing	L_{kr}, mm	τ_{lok}, MPa	$\sigma_{max.}$, MPa
After curing	1.006	1.3025	104.62

The process of destruction of the composite structure components as well as the composite itself should be complemented by the analysis of the influence not only of the load, but also of the

atmospheric (operational) factors, which complement the sequential accumulation of damage. Having a well-crosslinked (hardened) laminate we can determine the influence [14] of aggressive factors (such as sulphur di- and trioxide SO_2 and SO_3, nitrogen oxides and carbon oxides), which in combination with moisture are inorganic acids.
Also, during aging (which is a process of structural changes that occur in the polymer under the influence of long-term external factors) under natural climatic conditions, it is most often difficult to distinguish which factor has the dominant influence, as they act simultaneously. All the above-mentioned chemical transformations are very complex and often proceed simultaneously.

5. Conclusions

This paper presents the microstructure and mechanical properties of a cold sprayed Ti-6Al-4V structure for the structure of a composite (laminate) for application in additive manufacturing on hydraulic components. A model for estimating the strength of a fibrous composite based on the critical micro-volume, taking into account the distribution of strength properties and the degree of hardening during the laminate curing process using the vacuum bag method is described. The model has been validated with literature examples and experimental data. The non-linear internal heat source and heat transfer process cause non-uniformity in temperature and cure inside the epoxy part. This work is therefore an introduction and at the same time an innovative method that allows further insight into the epoxy resin curing process, which can improve the mechanical and operational properties of the finished element by reducing deformations and residual stresses during the curing process.

References

[1] Lakho, Dildar Ali, Donggang Yao, Kyonghoon Cho, Muhammad Ishaq, and Youjiang Wang. " Study of the Curing Kinetics toward Development of Fast-Curing Epoxy Resins ". *Polymer-Plastics Technology and Engineering* 56, no. 2 (2017): 161-170.
[2] Bereska, Bartłomiej, Jolanta Iłowska, Krystyna Czaja, and Agnieszka Bereska. "Hardeners for epoxy resins." *Przemysł chemiczny* 93, no. 4 (2014): 443-448.
[3] Zhang, J., Y.C. Xu, and P. Huang. “Effect of cure cycle on curing process and hardness for epoxy resin.” *eXPRESS Polymer Letters* 3, no. 9 (2009): 534–541.
[4] Stoltenhoff, T., J. Voyer and H. Kreye. “Cold Spraying - state of the art and applicability.” Paper presented at the International Thermal Spray Conference - ITSC 2002, Essen, Germany, March 4-6, 2002.
[5] Królikowski, Wacław. *Polymer structural composites* / *Polimerowe kompozyty konstrukcyjne*. 1st edition. Warsaw, PWN Publishing House, 2017.
[6] ***. “Composite production method using a vacuum bag.” / "Metoda produkcji kompozytów z użyciem worka próżniowego." April 9, 2012. Accessed February 16, 2020. http://laminaty-trax.blogspot.com/2012/04/metoda-produkcji-kompozytow-z-uzyciem.html.
[7] RYMATEX. Product Catalogue.
[8] Gutans, Juris, Piotr Zagulski, Druvis Verzemnieks, and Martins Kleinhofs. "Failure Model for Unidirectional Composite Element." *Composites the Theory and Practice* 22, no. 2 (2022) 58-61.
[9] Impact Innovations GmbH. Accessed November 6, 2023. https://impact-innovations.com.
[10] Chatys, Rafał, Martins Kleinchofs, Aleksander Panich, and Krzysztof Piernik. "Forecasting the Strength of Reinforced Polymer Composite Using Statistical Analysis Method." Paper presented at the 24th International Conference "Engineering Mechanics 2018", Svratka, Czech Republic, May 14-17, 2018.
[11] Chatys, Rafał, and Łukasz Jan Orman. “Technology and properties of layered composites as coatings for heat transfer enhancement." *Mechanics of Composite Materials* 53, no. 3 (July 2017): 351–360.
[12] Xiong, Xuhai, Rong Ren, Siyang Liu, Shaowei Lu, and Ping Chen. "The curing kinetics and thermal properties of epoxy resins cured by aromatic diamine with hetero-cyclic side chain structure.” *Thermochimica Acta* 595 (November 2014): 22–27.
[13] German, Janusz. *Basics of mechanics of fibrous composites* / *Podstawy mechaniki kompozytów włóknistych*. Cracow, AGH University Press, 1996.
[14] Szumniak, J., Z. Smoczyński, and K. Szcześniak. "Armament and military equipment polymer composite ageing.” / "Starzenie polimerowych kompozytów uzbrojenia i sprzętu wojskowego." *Zeszyty Naukowe WSOWL* 159, no. 1 (2011): 271-285.